

## OPTIMIZING HIGH PRESSURE CHEMICAL OXYGEN-IODINE LASERS

David L. Carroll

*University of Illinois, 306 Talbot Lab, Urbana, Illinois 61801*

### Abstract

The Blaze II chemical laser model was baselined to existing oxygen-iodine research assessment and device improvement chemical laser (RADICL) gain data. Subsequent Fabry-Perot power calculations with Blaze II were an average of 33% higher than the corresponding stable resonator power data. With the Blaze II model baselined to RADICL gain data, a genetic algorithm (GA) was used to predict optimal flow conditions and device configuration at high total pressures in the range of 100-250 Torr. This is the first known application of the genetic algorithm technique for optimizing the performance of a laser system. This modeling indicates that it should be possible to obtain significant power levels ( $> 19$  kW) with the RADICL device under high pressure operating conditions. The optimal flow conditions maximized the  $\text{Cl}_2$  flow rate into the  $\text{O}_2(^1)$  generator. It may be possible to improve high pressure RADICL performance by increasing the number of large injectors and decreasing their spacing. The use of nitrogen as a secondary diluent was investigated; a comparison of data with calculations suggest that there may be missing  $\text{N}_2$  kinetics in the existing rate package. Reactions which are recommended for investigation are the deactivation of  $\text{O}_2(^1)$ ,  $\text{O}_2(^1)$  and  $\text{I}^*$  by  $\text{N}_2$ .

### I. Introduction

The typical chemical oxygen-iodine laser (COIL) utilizes an energy transfer from the singlet delta excited state of oxygen  $\text{O}_2(^1)$  directly and indirectly to  $\text{I}_2$  to dissociate the iodine molecule. This process is followed by an energy transfer from other  $\text{O}_2(^1)$  molecules to the liberated iodine atoms, thus providing the energy for the atomic iodine laser transition of interest. A number of papers have investigated issues associated with the operation of chemical oxygen-iodine laser (COIL) systems. While there are numerous COIL related papers, a good summary of COIL technological development is presented in Ref. 1. However, only recently have researchers studied the effects of high pressure operation on small signal gain, iodine dissociation, the extent of mixing, power and system performance. The motivation for such research is that, if the total pressure of a COIL device can be increased significantly while maintaining the device's nominal performance, then it may be possible to reduce the size of pressure recovery systems. Carroll<sup>2</sup> addressed the issues of the small signal gain, power, and system performance when the total pressure of the flow is increased significantly. Barmashenko<sup>3</sup> addressed similar issues at much lower operating pressures. Tate<sup>4</sup> has performed detailed two-dimensional gain measurements of a COIL flow field as the total pressure of the flow was increased up to around 130 Torr. Helms<sup>5</sup> recently investigated the effects of total pressure on the iodine dissociation up to 100 Torr and Scott<sup>6</sup> has discussed the effects of total pressure on penetration and mixing characteristics.

To better understand how to optimize the performance of a high pressure COIL device, the effects of increased total pressure on mixing, kinetics, gain and power were investigated in Ref. 2 using the Blaze II computer model.<sup>7</sup> This modeling provided insights about the interactions between flow rates, kinetics, mixing, and pressure on COIL performance. The next step in the RADICL optimization process was to expand the search to higher pressure operating conditions using different geometries with the goal of using qualitative predictions to help guide future experiments.

### II. Baselineing Blaze II Model to Gain Data

Since high pressure COIL experiments have been performed with the RADICL nozzle at Phillips Laboratory, these modeling investigations focused on that nozzle. A top view schematic of the RADICL device is shown in Fig. 1. A side view schematic of the RADICL nozzle and laser cavity section are shown in Fig. 2. Details of the RADICL device can be found in Refs. 8 and 2.

The previous COIL modeling of the RADICL device was performed by matching power calculations from a Fabry-Perot model (Blaze II) to stable resonator power data.<sup>2</sup> While this is an acceptable approach when no other data (such as gain data and/or Fabry-Perot data) are available, it is generally believed that matching a model to gain data is a better method because the complicated mode-media interaction effects of lasing do not have to be modeled (a difficult and computationally expensive task if physical optics are included). With the recent availability of gain data for the RADICL device,<sup>4</sup> an effort was undertaken to baseline the Blaze II model<sup>7</sup> to this gain data.

Blaze II models three streams, a primary flow (pri) containing the  $\text{O}_2(^1)$ , a secondary flow (sec) containing the  $\text{I}_2$  fuel, and the mixed flow, Fig. 3. All properties are considered to be uniform in each stream in the transverse directions  $y$  and  $z$ , but vary as a function of the flow direction  $x$ . Since the flow properties are uniform in the transverse directions  $y$  and  $z$ , the gain in the mixed stream has no variation in the  $y$  and  $z$  directions. However, RADICL gain data<sup>4</sup> clearly show variation in the transverse direction  $y$ . Three-dimensional CFD modeling calculations for RADICL also predict this variation.<sup>9</sup> Thus, a question which naturally

arises is, what is an appropriate way to compare gain predictions from the uniform mixed stream of Blaze II (which also has two zero-gain regions in the primary and secondary streams) with experimental data?

The available gain data presented three natural choices for comparison with Blaze II predictions: a centerline scan, peak values of vertical scans and an average of vertical scans. Comparing the model with the centerline scan data is not appropriate for under penetrated cases where the gain is very low at the centerline, but may be relatively high in other portions of the flow. While the predicted gain in the mixed region may compare favorably with the peak data values, if the predicted mixed region is not large enough, then comparing strictly with peak data may not be representative of the gain data as a whole. Thus, two comparisons were made to judge the agreement between data and the model. First, the peaks of the vertical scans were compared with the gain predicted by Blaze II in the mixed region. Second, the average of the vertical scans were compared with the average gain predicted by Blaze II across the gain cell. The average predicted gain ( $g_{avg}$ ) is taken to be the gain in the mixed flow ( $g_{mixed}$ ) multiplied by the fraction of the flow which is mixed at any position  $x$ ,

$$g_{avg} = g_{mixed} [ \ / (S/2) ] \quad (1)$$

where  $\$  is the transverse width of the mixed stream, and  $S$  is the spacing between the injectors, Fig. 3.

With the availability of new rate data for  $I_2^*+M \rightarrow I_2+M$  deactivation reactions,<sup>10,11</sup> the kinetic package was updated before any calculations were made, Table 1. It is important to note that rates  $k_{16}$ - $k_{18}$  are significantly different than in previously reported rate packages.<sup>1,2,3,12</sup> The values of the  $I_2^*+O_2(^1\ \ )$  and  $I_2^*+H_2O$  deactivation rates are an order of magnitude smaller than the previous mechanisms indicate.

Early efforts to match RADICL gain data using the baseline to power data established in Ref. 2, gave reasonable agreement with some peak gain data, but the predicted average gains were all significantly below those of the averaged data. This trend is an indication that the mixing predicted by Blaze II using the old baseline to power data was too slow. Recent CFD calculations by Madden et al.<sup>9</sup> also predict faster mixing than these early Blaze II computations. With these indicators of faster mixing, the perspective of the mixing was switched from a single slit nozzle mixing scheme (used in Ref. 2) to an array nozzle mixing scheme to enhance the rate of mixing in the model. For RADICL, the array nozzle mixing scheme improves the rate of mixing because the length scale over which the gases must diffuse is significantly smaller. The length scale appropriate for an array nozzle mixing scheme in RADICL is the injector jet separation  $S$  (0.085" for the large injectors and 0.0425" for the small injectors). The length scale appropriate for the single slit nozzle mixing scheme is the nozzle height  $2Y_0$  (0.401" which expands to more than 1.20"). Clearly, the time it takes for gas to diffuse between injectors will be much less than the time it would take to diffuse across the nozzle. The array nozzle mixing scheme is illustrated in Figs. 3 and 4 (consider  $S$  in these figures to be the spacing between large injectors  $S_{large}$ ).

There was a substantial increase in mixing resulting from the use of an array nozzle mixing scheme rather than the single slit nozzle mixing scheme used in Ref. 2. This increase eliminated the need for a diffusion coefficient multiplier ( $DCM$ ) as large as that suggested by Driscoll.<sup>2,13</sup> However, it was still necessary to increase the primary and secondary laminar diffusion coefficients by approximately 50% to obtain a reasonable match between the predicted average gain and the average gain data (discussed below). An a priori estimate of the  $DCM$  can be made using surface stretching concepts. Since the jet penetrating into the primary cross flow is approximately cylindrical, it is possible to argue that the mixing surface is stretched from a planar sheet to a cylindrical sheet. In a single cell of the array nozzle mixing scheme in Blaze II only half of a large injector is considered, Figs. 3 and 4. A planar surface in the flow direction  $x$  has a contact distance between the primary and secondary streams equal to the diameter of the jet  $D$ . If this planar surface is stretched cylindrically it will have a contact distance of  $D / 2$  around the perimeter of half of the large injector. Thus, the surface stretching factor is  $/ 2 = 1.6$ . The  $DCM$  is effectively the amount of surface stretching, therefore the a priori estimate of the  $DCM$  is 1.6.

While there is considerable uncertainty in the yield  $\{Y = [O_2(^1\ \ )] / [Total\ O_2]\}$  and water vapor flow rate for different flow conditions, the best estimates<sup>14</sup> for the yield and  $H_2O$  flow rates as a function of the total primary flow rate are used in the Blaze II calculations. The best estimates for the yield and  $H_2O$  flow rate are approximated by

$$Y = 0.365 + 0.394 \log \dot{x}(Cl_2)_0 + \dot{x}(He)_{pri} \quad \text{and} \quad \dot{x}_{H_2O}[\text{moles/s}] = 0.0379 + 0.0475 \log \dot{x}(Cl_2)_0 + \dot{x}(He)_{pri} \quad (2)$$

where  $\dot{x}_i$  is the molar flow rate of species  $i$ .

Figure 5 shows good agreement between Blaze II and data for the nominal low pressure flow conditions,  $\beta = 3$ ,  $\beta = 0.017$ ,  $P_t = 75$  Torr, where the diluent ratio  $\beta = \dot{x}(He)_{pri} / \dot{x}(Cl_2)_0$ , the titration ratio  $\beta = \dot{x}I_2 / \dot{x}O_2 = \dot{x}I_2 / U \dot{x}(Cl_2)_0$ ,  $U$  is the utilization of the  $Cl_2$  flow rate into the oxygen generator, and  $P_t$  is the total pressure of the primary flow. The  $DCM$  used to obtain the predicted curves in Fig. 5 was 1.6, the a priori assumed value. Increasing the  $DCM$  speeds up the mixing which has two primary effects on the predicted gain curves. First, increasing the  $DCM$  shifts upstream the point at which the mixed and average curves meet (the point of fully mixed flow), and second, decreases the separation between the mixed and average predicted curves. A  $DCM$  of 1.6 gave the best overall agreement between the separation of peak gain data and average gain data for all of the available gain data (a total of three well penetrated and two under penetrated cases). Increasing the  $DCM$  above 1.6 tended to

produce complete mixing in a highly under penetrated low pressure case; this was in very poor agreement with the data and the corresponding power calculation was too high. Decreasing the *DCM* below 1.6 tended to produce too little mixing in a slightly under penetrated high pressure case; this was in poor agreement with the data and the corresponding power calculation was too low. Thus, it was felt that a value of 1.6 for *DCM* gave the best overall match to gain and power data.

Using the best estimates (discussed above) for yield and water flow rate (0.074 moles/s), Fig. 6 shows that Blaze II overpredicts the gain data for high pressure, slightly under penetrated flow conditions ( $\beta = 10$ ,  $\alpha = 0.027$ ,  $P_t = 130$  Torr). The data illustrated in Figs. 5 and 6 have an error bar of  $\pm 0.0015 \text{ cm}^{-1}$ .<sup>4</sup> The natural question which arises is, why is the low pressure case fairly well predicted (Fig. 7) while there is significant disagreement with the high pressure case (Fig. 6)? The answer to this question is not known for certain, but is believed to be a consequence of one or a combination of the uncertainties in the yield and water flow rate estimates, and/or that the rate constant  $k_{J8}$  may still be too small as suggested in Ref. 2. From a lack of a better choice, the estimated yield and water vapor flow rates given by Eq. (2), and the measured rate for  $k_{J8}$  are used as the baseline to RADICL gain data for all subsequent calculations.

At this point, the Blaze II model was considered to be baselined to RADICL gain data and the next step was to compare predicted Fabry-Perot powers with stable resonator data. All of the power calculations in this study were made for an outcoupler having a 91% reflectivity with a 1.0% diffractive loss and a 0.5% absorption/scattering loss, and a total reflector having a 99.5% reflectivity with a 0.5% absorption/scattering loss. The 1% diffractive loss was included in the outcoupler's loss term based on results by Hon et al.<sup>17</sup> Distributed loss was not included in any of these calculations. The size of the mirror aperture was 4 cm (the same size as that used in the existing experimental data) for all power calculations in this study; it was found that with Fabry-Perot calculations, typically 95-100% of the power was extracted within 4 cm of the leading edge of the mirrors, therefore increasing the mirror size beyond 4 cm should not significantly improve the predicted power. For the nominal flow condition case shown in Fig. 5, the measured power was 6.1 kW and the predicted power was 8.9 kW. For the high pressure case shown in Fig. 6, the measured power was 6.7 kW and the predicted power was 6.6 kW (with the best estimate of 0.074 moles/s for the water flow rate). For the five cases which were matched to gain data, the predicted power was an average of approximately 33% higher than the actual measured power (or 4/3 times the measured power). Conversely, actual measured stable resonator powers were an average of 75% ( $3/4$ ) of the predicted Fabry-Perot powers. Thus, any predicted powers discussed later are assumed to be 33% too large, and that likely measured powers for flow conditions which have not been experimentally tested will be assumed to be 75% of the predicted values. Based on a comparison of the above predicted powers with measured powers, the power predictions of Blaze II must be considered qualitative in nature.

### **III. Optimizing High Pressure Performance**

With the Blaze II model baselined to RADICL gain data, a genetic algorithm<sup>18</sup> (GA) was implemented to optimize laser performance as a function of the flow rates [ $\dot{x}(\text{Cl}_2)_0$ ,  $\dot{x}(\text{He})_{\text{pri}}$ ,  $\dot{x}(\text{I}_2)$ ,  $\dot{x}(\text{He})_{\text{sec}}$ ], mirror position and nozzle configuration. The four flow rates represent four parameters, the mirror location another, and there are three relevant nozzle configuration parameters that can be readily adjusted in the RADICL device. The adjustable nozzle geometry factors are the addition of a spacer plate between the injectors and the throat (increasing the subsonic section of the flow), the throat height (which was chosen as 0.353", 0.56", 0.65", or 0.75"), and the laser cavity expansion angle which can be varied from 0° to 5° (these ramps were set to 3° for nominal operating conditions). This is the first known application of the genetic algorithm technique for optimizing the performance of a laser system (chemical, solid-state, or gaseous).

One of the objectives of the GA optimization search was to determine if there were any systematic trends associated with the parameters, e.g., a priori, it is anticipated that the highest powers will always be associated with the highest allowable chlorine flow rates  $\dot{x}(\text{Cl}_2)_0$  [higher initial chlorine flow results in more oxygen flow and consequently more  $\text{O}_2(^1\Delta_g)$ ]. The 8 parameters were assigned realistic ranges for high pressure operating conditions, Table 2. The maximum values of the gas flow parameters are based on estimates of the current limitations of the RADICL device.<sup>19</sup> The GA search space was restricted to high pressure conditions having a primary He flow rate of 4.5-7.5 moles/s and an iodine flow rate in the range of 12.0-19.0 mmoles/s, Table 2. The lower limit of 4.5 moles/s of primary He was chosen to keep the total pressure above 100 Torr. The search space did not include iodine flow rates less than 12.0 mmoles/s because Helms<sup>19</sup> experienced power instabilities with RADICL at titration ratios less than 0.010 (12 mmoles/s of  $\text{I}_2$  combined with a  $\text{Cl}_2$  flow rate of 1.3 moles/s corresponds to  $\beta = 0.011$ ). The 8 parameters were discretized and then translated into a binary string of length 23, Table 2. There are approximately 8 million ( $=2^{23}$ ) possible permutations of this parameter space. The successful use of the GA technique for searching large chemical laser parameter spaces was demonstrated for the first time by Carroll.<sup>2</sup>

The optimization search showed the anticipated trend of maximizing the  $\text{Cl}_2$  (or equivalently the  $\text{O}_2$ ) flow rate, along with minimizing the  $\text{He}_{\text{pri}}$  flow rate (which lowers the pressure and He deactivation in the flow, while increasing the diffusional mixing rate). For high  $\text{Cl}_2$  flow rate conditions, minimizing the titration ratio to values of  $\beta = 0.010$  maximized the power (discussed below). The search in the high pressure flow regime (100-250 Torr) showed a preference for maximizing the penetration by maximizing the secondary He flow rate. Optimal powers under high pressure conditions tended to occur with the

mirror leading edge location further downstream; this may reflect the fact that there is more mixed flow further downstream. It should be pointed out that these predictions were made using a Fabry-Perot resonator model, while data are generally taken with a stable resonator; it is possible that the use of a stable resonator may change the conclusion of moving the resonator edge further downstream because of the upstream-downstream coupling inherent in a stable resonator. The search indicated that the addition of a spacer plate tended to decrease the laser performance; this is an indication that too much deactivation occurs in the subsonic region when a spacer plate is added and suggests that it may be beneficial to reduce the spacing between the injectors and the throat. The larger throat heights of 0.65" and 0.75" were preferred; this trend is not surprising because the plenum pressures were lower in these cases (resulting in faster diffusive mixing) and the high flow rate conditions lead to higher velocities which lower the  $O_2(^1\Delta_g)$  transport losses. The larger expansion angles of 4.5° and 5.0° were preferred; this is believed to be a consequence of the resulting lower temperatures in the flow. However, there was typically only a 1-2% improvement in power when the expansion angle was increased from 3.0° to 5.0°. It is important to point out that conclusions based on these trends may only be appropriate for the flow regime studied in Table 2.

The GA found an optimal set of the parameters with a predicted power of 26.5 kW; since the predicted powers using the baseline to gain data were approximately 33% higher than were measured powers (discussed above), the likely measured power should be roughly 19.9 kW. The parameter set that provided the optimal power had flow rates of 1.3 moles/s of  $Cl_2$ , 4.5 moles/s of  $He_{pri}$ , 12.0 mmoles/s of  $I_2$ , 2.25 moles/s of  $He_{sec}$ , the mirror leading edge at 12.2 cm, no spacer plate, a throat height of 0.75", and a 4.5° angle of divergence in the cavity. The total pressure of this flow was approximately 100 Torr. The diluent ratio for this case is  $\lambda = 3.5$  and the titration ratio is  $\tau = 0.011$ .

#### **IV. Nitrogen Secondary Diluent Predictions**

For the purposes of commercial and economically viable chemical oxygen-iodine lasers, the use of nitrogen as a diluent was investigated because it is significantly less expensive than helium. A calculation was performed for high pressure (130 Torr total pressure) conditions with  $\lambda = 10$  and  $\tau = 0.024$  and a secondary flow rate of  $N_2$  of 0.652 moles/s. Because of the availability of data, only the secondary diluent was changed, i.e. no data were available using  $N_2$  as the primary diluent, therefore helium was still used as the diluent in the primary stream. It should be noted that the data presented in Section II were taken with a reduced volume in the transition duct region (between the  $O_2$  generator and the injectors). The reduced volume increases the flow velocity, which consequently decreases the transport losses and delivers a higher yield to the actual laser cavity; this produces higher power levels. The  $N_2$  and He data discussed in this section were taken with the larger volume transition duct. Since the Blaze II model as described in Ref. 2 was baselined to the larger volume power data, the calculations in this section will use the old baseline for comparison with the large volume  $N_2$  power data. Since we will compare power calculations from a model which was baselined to power data, there is no need for a power adjustment factor as there was for results discussed in Sections II and III. The  $N_2$  calculation includes the use of reaction 20, Table 1.

The  $N_2$  secondary calculation had a significant gain in the mixed flow and Blaze II predicts a power of 3902 Watts. The experimentally measured power with  $N_2$  as the secondary diluent was 2590 Watts. Since we are using the model baselined to power data, it is reasonable to expect no more than roughly a 20% disagreement between the model and data when only the secondary diluent is changed (less than 10% of the total molar flow rate). The fact that the  $N_2$  power calculation was significantly larger (51%) than measured data suggests that there may be missing  $N_2$  kinetics in the existing rate package. Reactions which are recommended for investigation are the deactivation of  $O_2(^1\Delta_g)$ ,  $O_2(^1\Sigma_g^-)$  and  $I^*$  by  $N_2$ .

#### **V. Summary and Discussion**

The Blaze II code was baselined to RADICL peak and average gain data (rather than power data). New rate data for  $I_2^*+M$  and  $I_2+M$  deactivation reactions were used and the rate of mixing was increased in the baselining procedure. Good agreement with peak gain data and average gain data was obtained with Blaze II for a low pressure case. Blaze II over predicted higher pressure gain data; this over prediction is believed to be primarily a consequence of uncertainties in the water vapor flow rate and the yield, and/or too small a value for  $k_{J8}$  as suggested in Ref. 2. Best estimates of the yield and water flow rate were used for the Blaze II baseline to gain data. Subsequent Fabry-Perot power calculations with Blaze II were an average of 33% higher than the corresponding stable resonator power data.

Since reduced kinetic mechanisms are essential for CFD calculations (to minimize run time), the rates listed in Table 1 were tested in Carroll's<sup>2</sup> reduced 13 species/10 reaction and 8 species/8 reaction mechanisms. The agreement between these reduced mechanisms and the full mechanism was excellent; thus, these reduced mechanisms are recommended for use in CFD modeling.

With the Blaze II model baselined to RADICL gain data, a genetic algorithm (GA) was used to predict optimal flow conditions and device configuration at high total pressures in the range of 100-250 Torr. This is the first known application of the genetic algorithm technique for optimizing the performance of a laser system (chemical, solid-state, or gaseous). An optimal set of flow conditions and geometry was found with a predicted power of 26.5 kW; since the baselined predicted powers were approximately 33% higher than were measured powers, the likely measured power should be roughly 19.9 kW. The total

pressure of this flow is approximately 100 Torr. The optimal flow conditions maximized the Cl<sub>2</sub> (or equivalently the O<sub>2</sub>) flow rate. The power was maximized by minimizing the primary He flow rate to a level which still maintained a high stagnation pressure of 100 Torr; lower He flow reduces deactivation by He and lower pressure improves diffusional mixing. For high Cl<sub>2</sub> flow rate conditions, minimizing the titration ratio to values of 0.010 maximized the power. Maximizing the secondary He flow improved the power by increasing the penetration and mixing. The predicted Fabry-Perot power was maximized by moving the resonator leading edge downstream; this conclusion may not be valid for a stable resonator because of the inherent upstream-downstream mode-media coupling in a stable resonator. Power was optimized with larger throat sizes and with no additional spacer plate between injectors and throat; this suggests that it may be possible to improve power with larger throats and/or decreasing the distance between the injectors and the throat. An increase from 3° to 4.5° in the constant expansion angle cavity section is recommended, but is predicted to improve the power by only 1-2%. It is important to point out that conclusions based on these trends may only be appropriate for the studied flow regime. Most importantly, this modeling indicates that it should be possible to obtain significant power levels (> 19 kW) with the RADICL device under high pressure operating conditions.

Can further improvements be made to the high pressure performance design? Figures 5 and 6 show that complete mixing is obtained in the low pressure conditions (the mixed region and average gain curves overlap at  $x = 11$  cm), but not in the high pressure conditions (the mixed region and average gain curves never overlap in the laser cavity). Detailed CFD calculations also show this behavior of complete mixing in the low pressure case, but incomplete mixing at high pressure.<sup>9</sup> The geometrical parameters investigated above were restricted to the readily alterable hardware modifications designed into the RADICL device; these geometrical parameters alone did not tend to improve the mixing rate under high pressure conditions. However, one way to enhance the mixing at high pressure is to decrease the spacing  $S$  between the large injectors; this will decrease the distance over which the gases must diffuse and thus decrease the flow distance to obtain complete mixing. Thus, it may be possible to improve high pressure RADICL performance by increasing the number of large injectors and decreasing their spacing  $S$ .

For the purposes of commercial and economically viable chemical oxygen-iodine lasers, the use of nitrogen as a secondary diluent was investigated because it is significantly less expensive than helium. Using the prior baseline to power data, the fact that an N<sub>2</sub> power calculation was significantly larger than measured data suggests that there may be missing N<sub>2</sub> kinetics in the existing rate package. Reactions which are recommended for investigation are the deactivation of O<sub>2</sub>(<sup>1</sup>), O<sub>2</sub>(<sup>1</sup>) and I\* by N<sub>2</sub>.

#### Acknowledgements

This work was supported by the Air Force through Logicon/RDA subcontract 907629. Many thanks to R. Tate and C. Helms for the RADICL data, and to G. Hager, K. Truesdell, D. Plummer, L. Sentman, W. Solomon and T. Madden, for several useful conversations.

#### References

- <sup>1</sup>Truesdell, K. A., Lamberson, S. E., and Hager, G. D., AIAA Paper 92-3003, 1992.
- <sup>2</sup>Carroll, D. L., *AIAA J.*, Vol. 33, 8, 1995, pp. 1454-1462.
- <sup>3</sup>Barmashenko, B. D., Elmor, A., Lebiush, E., and Rosenwaks, S., AIAA Paper 94-2434, 1994.
- <sup>4</sup>Tate, R. F., Hunt, B. S., Helms, C. A., Hager, G. D., and Truesdell, K. A., AIAA Paper 94-2438, 1994.
- <sup>5</sup>Helms, C. A., Shaw, J., Hager, G.D., Truesdell, K.A., Plummer, D.N. and Copland, R.J., AIAA Paper 94-2437, 1994.
- <sup>6</sup>Scott, J. E., Shaw, J. L. R., Truesdell, K. A., Hager, G. D., and Helms, C. A., AIAA Paper 94-2436, 1994.
- <sup>7</sup>Sentman, L. H., Subbiah, M., and Zelazny, S. W., "Blaze II: A Chemical Laser Simulation Computer Program," Bell Aerospace Textron, Buffalo, NY, T.R. H-CR-77-8, February 1977.
- <sup>8</sup>Crowell, P. G., and Plummer, D. N., "Simplified chemical oxygen iodine laser (COIL) system model," *Intense Laser Beams and Applications*, International Society for Optical Engineering, Vol. 1871, Los Angeles, CA, 1993, pp. 148-180.
- <sup>9</sup>Madden, T., Carroll, D., and Solomon, W., "CFD Investigation of High Pressure Performance of COIL Devices," *International Conference on Lasers '95*, Charleston, SC, Dec. 4-8, 1995.
- <sup>10</sup>Heaven, M. C., private communication, Emory Univ., July 1994.
- <sup>11</sup>Heaven, M. C., "Studies of Energy Transfer Processes of Relevance to Chemically and Optically Pumped Lasers," Emory University AFOSR/NR F49620-92-J-0073, Dec. 1994.
- <sup>12</sup>Perram, G.P., and Hager, G.D., "The Standard Chemical Oxygen-Iodine Laser Kinetics Package," AFWL-TR-88-50, Oct. 1988.
- <sup>13</sup>Driscoll, R. J., *AIAA J.*, Vol. 24, 7, 1986, pp. 1120-1126.
- <sup>14</sup>Plummer, D. N., private communication, Logicon/RDA, Albuquerque, NM, May 1995.
- <sup>15</sup>Cline, J. I., and Leone, S. R., *J. Phys. Chem.*, Vol. 95, 7, 1991, pp. 2917-2920.
- <sup>16</sup>Burde, D. H., Yang, T. T., and McFarlane, R. A., *Chem. Phys. Lett.*, Vol. 205, 1, 1993, pp. 69-74.
- <sup>17</sup>Hon, J., Plummer, D.N., Crowell, P.G., Erkkila, J., Hager, G.D., Helms, C.A. and Truesdell, K.A., AIAA Paper 94-2422, 1994.
- <sup>18</sup>Goldberg, D. E., *Genetic Algorithms in Search, Optimization and Machine Learning*, Addison-Wesley, Reading, MA, 1989.
- <sup>19</sup>Helms, C. A., private communication, Phillips Laboratory, Kirtland AFB, May 1995.

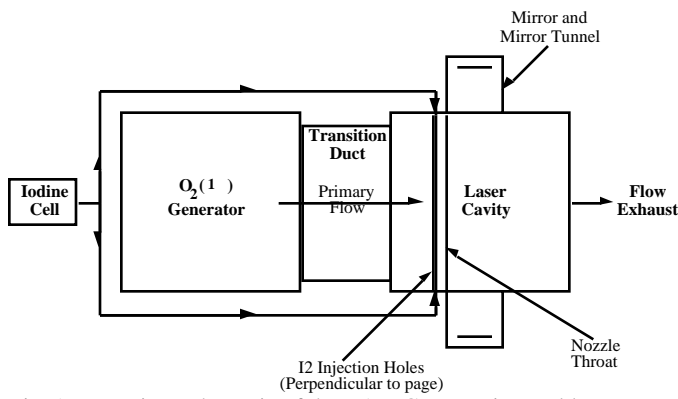


Fig. 1 Top view schematic of the RADICL experimental layout.

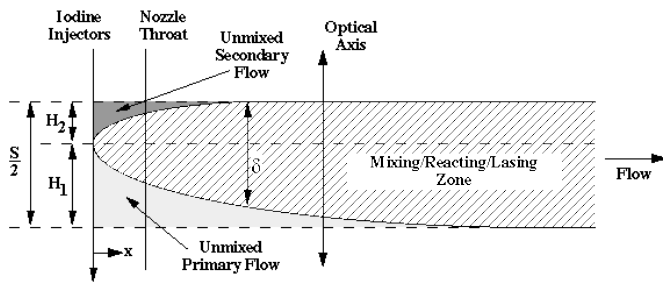


Fig. 3 Top view schematic of one cell in the Blaze II array nozzle laser mixing scheme. The  $I_2$  injectors are pointed out of the page at  $x=0$ . The lasing axis is in the  $z$  direction. The fraction of the flow which is mixed at position  $x$  is equal to  $x/(S/2)$ .

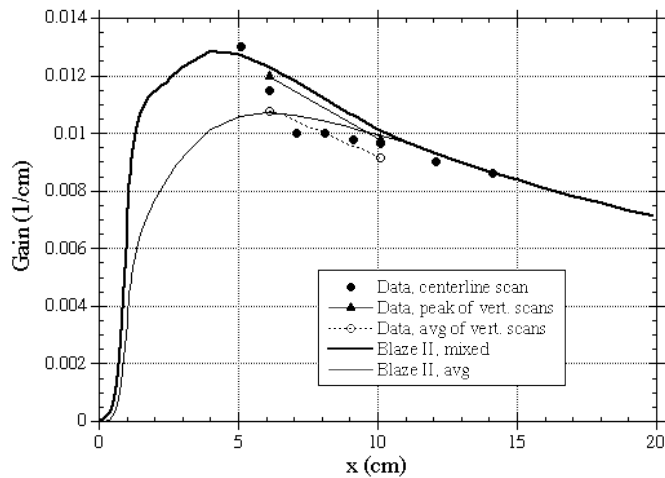


Fig. 5 Comparison of RADICL gain data with the profile predicted by Blaze II for low pressure ( $P=3$ ,  $\rho=0.017$ ) flow conditions. The yield was 48% and the water flow rate 0.052 moles/s for the Blaze II calculation.

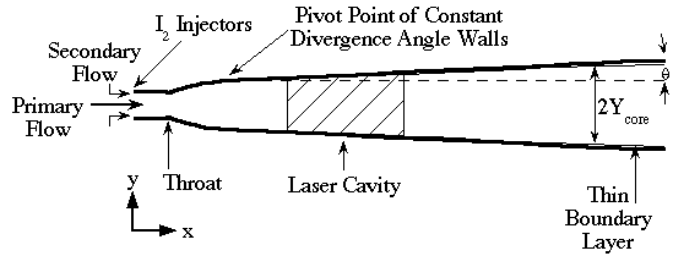


Fig. 2 Side view schematic of the RADICL nozzle showing nominal wall divergence angle, injector, throat, and laser cavity locations.

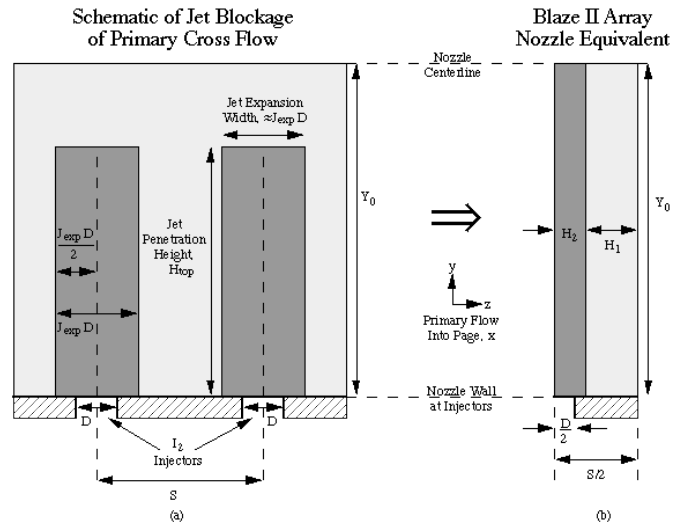


Fig. 4 Front view schematic of (a) the blockage of the primary cross flow by iodine injectors and (b) the Blaze II equivalent for an array nozzle laser. The injectors are oriented perpendicular to the primary flow. The optical axis (located further downstream) is parallel to the page in the  $z$ -direction.

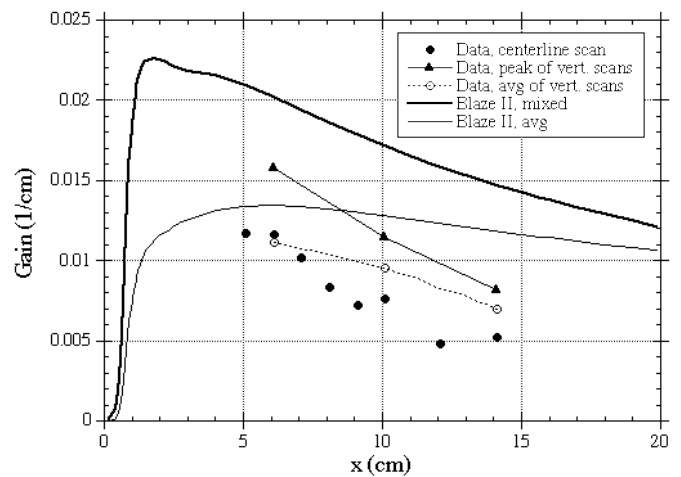


Fig. 6 Comparison of RADICL gain data with the profile predicted by Blaze II for high pressure ( $P=10$ ,  $\rho=0.027$ ) flow conditions. The yield was 67% and the water flow rate 0.074 moles/s for the Blaze II calculation.

**Table 1. Full oxygen-iodine reaction set; 35 reactions, 13 species: I, I\*, I<sub>2</sub>, I<sub>2</sub>\*, He, H<sub>2</sub>O, O<sub>2</sub> (<sup>1</sup>), O<sub>2</sub> (<sup>3</sup>), O<sub>2</sub> (<sup>1</sup>), Cl<sub>2</sub>, Cl, ICl, N<sub>2</sub>**

<i>k</i>							Rates, cm <sup>3</sup> /molecule-s
1	O <sub>2</sub> ( <sup>1</sup> )	+	O <sub>2</sub> ( <sup>1</sup> )	O <sub>2</sub> ( <sup>1</sup> )	+	O <sub>2</sub> ( <sup>3</sup> )	2.7e-17
2	O <sub>2</sub> ( <sup>1</sup> )	+	O <sub>2</sub> ( <sup>1</sup> )	O <sub>2</sub> ( <sup>3</sup> )	+	O <sub>2</sub> ( <sup>3</sup> )	1.7e-17
3	O <sub>2</sub> ( <sup>1</sup> )	+	O <sub>2</sub> ( <sup>3</sup> )	O <sub>2</sub> ( <sup>1</sup> )	+	O <sub>2</sub> ( <sup>3</sup> )	3.9e-17
4	O <sub>2</sub> ( <sup>1</sup> )	+	H <sub>2</sub> O	O <sub>2</sub> ( <sup>1</sup> )	+	H <sub>2</sub> O	6.7e-12
5	O <sub>2</sub> ( <sup>1</sup> )	+	Cl <sub>2</sub>	O <sub>2</sub> ( <sup>1</sup> )	+	Cl <sub>2</sub>	2.0e-15
6	O <sub>2</sub> ( <sup>1</sup> )	+	He	O <sub>2</sub> ( <sup>1</sup> )	+	He	1.0e-17
7	O <sub>2</sub> ( <sup>1</sup> )	+	O <sub>2</sub> ( <sup>3</sup> )	O <sub>2</sub> ( <sup>3</sup> )	+	O <sub>2</sub> ( <sup>3</sup> )	1.6e-18
8	O <sub>2</sub> ( <sup>1</sup> )	+	H <sub>2</sub> O	O <sub>2</sub> ( <sup>3</sup> )	+	H <sub>2</sub> O	4.0e-18
9	O <sub>2</sub> ( <sup>1</sup> )	+	Cl <sub>2</sub>	O <sub>2</sub> ( <sup>3</sup> )	+	Cl <sub>2</sub>	6.0e-18
10	O <sub>2</sub> ( <sup>1</sup> )	+	He	O <sub>2</sub> ( <sup>3</sup> )	+	He	8.0e-21
11	I <sub>2</sub>	+	O <sub>2</sub> ( <sup>1</sup> )	2I	+	O <sub>2</sub> ( <sup>3</sup> )	4.0e-12
12	I <sub>2</sub>	+	O <sub>2</sub> ( <sup>1</sup> )	I <sub>2</sub>	+	O <sub>2</sub> ( <sup>3</sup> )	1.6e-11
13	I <sub>2</sub>	+	O <sub>2</sub> ( <sup>1</sup> )	I <sub>2</sub> *	+	O <sub>2</sub> ( <sup>3</sup> )	7.0e-15
14	I <sub>2</sub>	+	I*	I	+	I <sub>2</sub> *	3.5e-11
15	I <sub>2</sub> *	+	O <sub>2</sub> ( <sup>1</sup> )	2I	+	O <sub>2</sub> ( <sup>3</sup> )	3.0e-10
16	I <sub>2</sub> *	+	O <sub>2</sub> ( <sup>3</sup> )	I <sub>2</sub>	+	O <sub>2</sub> ( <sup>3</sup> )	4.9e-12
17	I <sub>2</sub> *	+	H <sub>2</sub> O	I <sub>2</sub>	+	H <sub>2</sub> O	1.7e-11
18	I <sub>2</sub> *	+	He	I <sub>2</sub>	+	He	9.8e-12
19	I <sub>2</sub> *	+	Cl <sub>2</sub>	I <sub>2</sub>	+	Cl <sub>2</sub>	6.3e-12
20	I <sub>2</sub> *	+	N <sub>2</sub>	I <sub>2</sub>	+	N <sub>2</sub>	8.2e-12
21	I	+	O <sub>2</sub> ( <sup>1</sup> )	I*	+	O <sub>2</sub> ( <sup>3</sup> )	7.8e-11
22	I*	+	O <sub>2</sub> ( <sup>3</sup> )	I	+	O <sub>2</sub> ( <sup>1</sup> )	1.04e-10*exp(-401.4/T)
23	I	+	O <sub>2</sub> ( <sup>1</sup> )	I	+	O <sub>2</sub> ( <sup>3</sup> )	1.0e-15
24	I*	+	O <sub>2</sub> ( <sup>3</sup> )	I	+	O <sub>2</sub> ( <sup>3</sup> )	3.5e-16
25	I*	+	O <sub>2</sub> ( <sup>1</sup> )	I	+	O <sub>2</sub> ( <sup>1</sup> )	1.0e-13
26	I*	+	O <sub>2</sub> ( <sup>1</sup> )	I	+	O <sub>2</sub> ( <sup>1</sup> )	1.1e-13
27	I	+	I*	I	+	I	1.6e-14
28	I*	+	H <sub>2</sub> O	I	+	H <sub>2</sub> O	2.1e-12
29	I*	+	He	I	+	He	5.0e-18
30	I*	+	Cl <sub>2</sub>	Cl	+	ICl	5.5e-15
31	I*	+	Cl <sub>2</sub>	I	+	Cl <sub>2</sub>	8.0e-15
32	I*	+	ICl	I <sub>2</sub>	+	Cl	1.5e-11
33	I <sub>2</sub>	+	Cl	I	+	ICl	2.0e-10
34	Cl	+	ICl	I	+	Cl <sub>2</sub>	8.0e-12
35	I <sub>2</sub>	+	2I	I <sub>2</sub>	+	I <sub>2</sub>	3.6e-30

**Table 2. Genetic algorithm parameter search space for Blaze II.**

Parameter	$\dot{x}$ (Cl <sub>2</sub> ) <sub>0</sub> (moles/s)	$\dot{x}$ (He) <sub>pri</sub> (moles/s)	$\dot{x}$ I <sub>2</sub> (mmoles/s)	$\dot{x}$ (He) <sub>sec</sub> (moles/s)	Mirror Leading Edge (cm)	Spacer Plate Size (in)	Throat Height (in)	Cavity Divergence Angle (°)
Range	0.6 - 1.3	4.5 - 8.0	12.0 - 19.5	0.75 - 2.25	5.2 - 12.2	0.0, 0.25, 0.50, 0.75	0.353, 0.56, 0.65, 0.75	1.5 - 5.0
Increment	0.1	0.5	1.0	0.10	1.0	---	---	0.5
# of Possibilities	8	8	8	16	8	4	4	8
# of Binary Digits	3	3	3	4	3	2	2	3